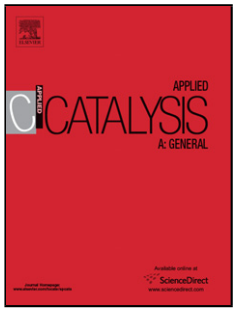

Title: Pd_3Sn nanoparticles on TiO_2 and ZnO supports as catalysts for semi-hydrogenation: Synthesis and catalytic performance

Authors: Shaun K. Johnston, Nikolay Cherkasov, Elena Pérez-Barrado, Atte Aho, Dmitry Y. Murzin, Alex O. Ibhadon, M. Grazia Francesconi

PII: S0926-860X(17)30305-8
DOI: http://dx.doi.org/doi:10.1016/j.apcata.2017.07.005
Reference: APCATA 16310

To appear in: *Applied Catalysis A: General*

Received date: 9-5-2017
Revised date: 20-6-2017
Accepted date: 5-7-2017

Please cite this article as: Shaun K.Johnston, Nikolay Cherkasov, Elena Pérez-Barrado, Atte Aho, Dmitry Y.Murzin, Alex O.Ibhadon, M.Grazia Francesconi, Pd3Sn nanoparticles on TiO2 and ZnO supports as catalysts for semi-hydrogenation: Synthesis and catalytic performance, Applied Catalysis A, Generalhttp://dx.doi.org/10.1016/j.apcata.2017.07.005

Pd_3Sn Nanoparticles on TiO_2 and ZnO Supports as Catalysts for Semi-hydrogenation: Synthesis and Catalytic Performance

Shaun K. Johnston,[a] Nikolay Cherkasov,[a,b] Elena Pérez-Barrado,[a,¥] Atte Aho,[c] Dmitry Y. Murzin,[c] Alex O. Ibhadon[d]* and M. Grazia Francesconi[a]*

a. School of Mathematics and Physical Sciences, Chemistry, University of Hull, Cottingham Road, Hull, United Kingdom, HU6 7RX.

b. School of Engineering, University of Warwick, Coventry, CV4 7AL, United Kingdom.

c. Laboratory of Industrial Chemistry and Reaction Engineering, Åbo Akademi University, Biskopsgatan 8, FI-20500 Turku/Åbo, Finland.

d. School of Engineering and Computer Science, Chemical Engineering, University of Hull, Cottingham Road, Hull, United Kingdom, HU6 7RX.

¥ Present address: School of Chemical and Physical Sciences, Keele University, Staffordshire, ST5 5BG, United Kingdom

To whom correspondence should be addressed: M.G.Francesconi@hull.ac.uk, A.O.Ibhadon@hull.ac.uk

Highlights

- Two new catalysts Pd_3Sn/TiO_2 and Pd_3Sn/ZnO were prepared via a one-pot procedure and the crystal structure of the catalytically active compound Pd_3Sn was studied.
- Pd_3Sn/TiO_2 and Pd_3Sn/ZnO catalyse the semi-hydrogenation of an acetylene alcohol with superior selectivity towards olefin compared to known Pd/ZnO and Pd/TiO_2 catalysts.
- Full reaction profiles show that Pd_3Sn/TiO_2 and Pd_3Sn/ZnO have well over 95% selectivity towards olefins at conversions of 90%.
- The catalysts can be used by the fine chemical industry to create high purity precursors in, for example, the synthesis of vitamins A and E.

Abstract

The two catalysts Pd_3Sn/TiO_2 and Pd_3Sn/ZnO were prepared via a one-pot procedure based on the "polyol method" with the addition of a capping agent (polyvinylpyrrolidone) to control the particle size distribution. The same procedure was used to prepare Pd/TiO_2 and Pd/ZnO for comparison. All four catalysts showed high activity and selectivity for the selective hydrogenation of 2-methyl-3-butyn-2-ol (MBY) to 2-methyl-3-buten-2-ol (MBE) in the liquid phase under identical conditions. However, Pd_3Sn/TiO_2 and Pd_3Sn/ZnO show selectivities to alkene significantly higher than that of the Pd catalysts. Specifically, the selectivity increases from 96.4% to 97.4% on TiO_2 support, and 96.2% to 97.6% on ZnO support, at 90% conversion. Transition electron microscopy shows nanoparticles evenly dispersed on the support, with mean particle sizes as low as 4.1 (±0.8) nm when Sn is incorporated into the catalyst. Unsupported Pd_3Sn was prepared using the same method and characterised by powder X-Ray diffraction followed by the Rietveld refinement. Pd_3Sn was found to be single-phase and isostructural to Pd metal with a face centred cubic unit cell.

Keywords: Alkyne, alkene, bimetallic, catalysis, palladium, selective hydrogenation, acetylene.

1. Introduction

Highly selective, active and environmentally-friendly catalysts are of prime importance for many areas of chemistry. In particular, the production of fragrances, pharmaceuticals, vitamins and agrochemicals relies on catalysts developed more than 60 years ago and requires significant improvement in terms of both environmental footprint and performance. An example of these catalytic reactions is selective hydrogenation, which involves, for example, the hydrogenation of a carbon-carbon triple bond to a double bond (semi-hydrogenation), avoiding over-hydrogenation to a single bond. Semi-hydrogenation is one of the critical steps in the synthesis of vitamins A and E, the fragrance compound linalool and other important compounds [1].

The semi-hydrogenation of 2-methyl-3-butyn-2-ol (MBY) to 2-methyl-3-buten-2-ol (MBE) (Figure 1) is an important starting reaction in industry [2] and is widely used as a model substrate to screen for activity and selectivity of catalyst materials in semihydrogenation reactions [3,4].

Palladium-based catalysts in semi-hydrogenation reactions are active and more selective than other platinum-group metals [5], but their selectivity towards alkene products is still limited due to over-hydrogenation to alkanes and other side reactions such as dimerization and oligomerization reactions [6]. To overcome this, a co-metal is often added to Pd to increase the selectivity. The co-metal can be added to the Pd catalyst as a surface poison, as is the case in the widely used Lindlar catalyst[7], in which $Pd/CaCO_3$ is modified by the addition of Pb. However, the use of lead for catalyst modification is subject to increasing environmental and product poisoning concerns [8].

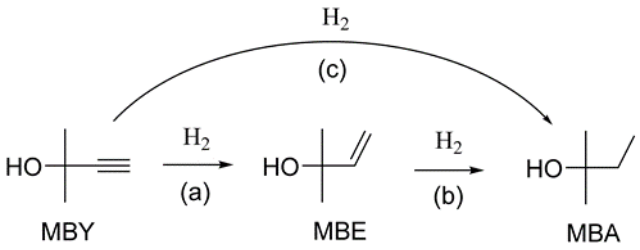

Figure 1. Reaction scheme of the hydrogenation of MBY to MBA. (MBY = 2-methyl-3-butyn-2-ol, MBE = 2-methyl-3-butene-2-ol and MBA = 2-methylbutan-2-ol.) For a selective semi-hydrogenation, steps (b) and (c) should be avoided.

Alternatively, a second metal (co-metal) can be incorporated to form a Pd-M alloy, which can take the form of core-shell, or a random or ordered alloy, depending on the synthetic procedure employed [9]. The

crystal structure of any resulting compounds formed between the two metals is often overlooked but can be very important. For example, work carried out on intermetallic compounds formed between Pd and Ga has shown that, depending on the stoichiometry and crystal structure of the compound formed between Pd and Ga, drastically different selectivities are achieved in gas phase acetylene hydrogenation [10]. Therefore, achieving phase purity, rather than mixtures of the various active compounds present throughout a catalyst, can also be considered of vital importance since different compositions formed between two metals can have different catalytic properties.

Many Pd-based alloy (bimetallic) materials have been tested in the literature as selective hydrogenation catalysts, utilising co-metals such as Ag [11,12], Au[13–15], Bi[8,16–18] , Co[19], Cu[20,21], Fe[22,23], Ni[23,24], Sn[25], Zn[26–29], Zr[30]. When forming an alloy with the second metal, selectivity can be enhanced by two main factors. Firstly, an increase in selectivity can occur due to changes in the electronic structure of Pd brought on by the presence of an additional metal, which can change the relative adsorption energies of alkyne and alkene bonds. This can result in a more favourable adsorption, and hence, the hydrogenation of alkyne, while disfavouring the adsorption and hydrogenation of alkene species [31]. Secondly, alloy formation can reduce the number and size of active site ensembles due to dilution of Pd [9,32]. This can inhibit secondary reactions that involve different functional groups, or neighbouring reactants to be adsorbed in close proximity to each other. Geometric effects should, however, have less impact on the semi-hydrogenation of acetylene alcohols as only one functional group is available for hydrogenation, although it may assist in preventing unwanted dimerisation reactions from taking place.

The co-metal of interest in this work is Sn, because Sn is non-toxic and is known to form a range of compounds with Pd. Known Pd-Sn binary alloys include $PdSn_4$, $PdSn_3$, $PdSn_2$, α- and β-Pd_3Sn_2, PdSn, Pd_2Sn and Pd_3Sn. We have focused our studies on Pd_3Sn, which is isostructural to Pd and hence makes for a better comparison to the catalytic performance of monometallic Pd.

Catalysts containing Pd-Sn alloys have already been used for electrooxidation [33,34], hydrogen peroxide synthesis [35], water denitration [36–38], and in the selective hydrogenations of unsaturated aldehydes [39,40], hexa- and butadienes [41–43], and gas phase acetylene [44]. In many of these reactions, high selectivity is achieved and attributed to the suppression of the adsorption of certain functional groups onto the catalyst due to the altered electronic structure, or to the formation of Pd-Sn bonds by the reduction of active site ensembles. The change in electronic structure of Pd on alloying with Sn has been shown by photoemission data to involve a valence charge transfer from Sn to Pd, and is most prominent when the alloys Pd_2Sn or Pd_3Sn are formed [45]. This charge transfer effect has also been shown to suppress the adsorption of C=C specifically, compared to Pd alone [40]. Furthermore, work carried out on compounds

such as PdGa has shown the benefit of isolated Pd sites (ensemble effect) in ordered alloys and intermetallic compounds in favouring the successive, stepwise hydrogenation of the acetylene bond rather than full hydrogenation to alkane [10,46–48].

However, in the current literature on Pd-Sn catalysts, there has been no attempt to achieve purity of the catalytically active Pd-Sn phase, hence mixtures of Pd/Sn monometallic and/or bimetallic phases are present in the catalyst [33,34,37–40,44]. This means that it is unclear which phases are responsible for any improved catalytic performance compared to monometallic Pd.

The aim of this work was to study the Pd-Sn alloy Pd_3Sn and assess the purity and crystal structure of the material. Furthermore, Pd_3Sn/TiO_2 and Pd_3Sn/ZnO catalysts were prepared and showed enhancement in the catalytic performance compared to Pd/TiO_2 and Pd/ZnO catalysts in the semi-hydrogenation of MBY.

2. Experimental

2.1. Materials

The metal precursors used in the catalyst preparation were palladium(II) acetylacetonate (99 %, Aldrich) and tin(II) acetyl acetate (99.9%, Aldrich). Zinc oxide (99.9%, 200 mesh powder, Alfa Aesar) and titanium(IV) oxide, rutile phase (powder, <5 μm, ≥99.9%, Aldrich) was used as support and polyvinylpirrolidone (PVP) (average mol. Wt. 40'000 g mol^{-1}, Sigma-Aldrich) was used as a capping agent. Acetone (laboratory reagent grade, Fischer Chemical), ethanediol (laboratory reagent grade, Fischer Chemical), n-hexane (GPR grade, VWR Chemicals) and deionised water were used as solvents without any pre-treatment. For the hydrogenation reactions, butan-1-ol (analytical reagent grade, Fisher Scientific) was used as internal standard for GC analysis. All chemicals were used as purchased.

2.2. Catalyst preparation

The method used for the preparation of the catalysts was adapted from a polyol method used by Cable and Shark [49] for the preparation of Pt_3Sn.

Firstly, appropriate stoichiometric amounts of the metal precursors, palladium acetylacetonoate and tin acetate, each in 100 mL ethylene glycol, were combined into the reaction vessel and either ZnO or TiO_2 support was added alongside PVP as capping agent (10 monomer mol% of total Pd and Sn). The amount of the support used was calculated to achieve 2 wt% Pd loading. The mixture was stirred under nitrogen gas flow at room temperature for at least 30 minutes to displace air before heating at reflux (469 K) for 1

hour. The mixture was cooled and the resulting brown/grey solid was obtained from the reaction mixture by centrifugation at 3500 rpm, washing alternately with acetone and deionised water (3 x 30 mL each) and dried at 353 K in air for 1 hour to yield a grey powder. The catalysts are stored in a vacuum desiccator until use.

Unsupported Pd_3Sn for structural characterisation was prepared using the same method with exclusion of the support and PVP.

2.3. Catalyst characterisation

Powder X-ray diffraction (PXRD) was carried out using a PANalytical Empyrean X-ray diffractometer using monochromatic Cu Kα1 radiation and line PIXcel detector, scanning in the 2θ range of 20-120°, step size 0.105° and step time 12000 seconds. Results were recorded using the instrument's built-in software. Rietveld refinement was performed using GSAS software with the EXPGUI interface [50].

Samples for transmission electron microscopy (TEM) were dispersed in ethanol using an ultrasonic bath and a drop of dispersion was deposited onto carbon-coated copper grids. Images were obtained using a Gatan Ultrascan 4000 digital camera with Digital Micrograph software, attached to a Jeol 2010 TEM instrument running at 200 kV. Nanoparticle size distributions were obtained studying 3-5 TEM microphotographs obtained from different areas of the catalyst sample, measuring the diameter of a total of 200-400 individual nanoparticles using Gatan Digital Micrograph software.

The total uptake of CO was measured with a Micromeritics AutoChem 2910 apparatus. Prior to a measurement, the catalyst was reduced in hydrogen with the following programme: flushing with helium at room temperature for 10 minutes, reduction in hydrogen at 573 K (10 K/min) for 120 minutes, flushing with helium at 573 K for 30 minutes and then returned to ambient temperature.

Palladium and tin content of the catalysts were determined using a Perkin Elmer Optima 5300DV emission inductively coupled plasma (ICP) spectrometer. The samples were dissolved in the solution of $HF/HCl/HNO_3$ in a 1/1/3 ratio, heated at 473 K for 10 minutes using microwave digestion system CEM MARS Xpress Plus, followed by the addition of the boric acid saturated aqueous solution to complex excess HF, and the vessels were heated again at 453 K for 10 minutes. The solutions were diluted with deionised water and analysed.

2.4. Hydrogenation reaction

For the hydrogenation procedure, freshly-prepared catalysts (between 5 and 50 mg, depending on the activity of the catalyst) and a hexane solution (100 mL) containing 0.741 g (10 mmol) of butan-1-ol used as an internal standard were transferred into a 250 mL 3-neck round bottom flask fitted with a silicone rubber septum, thermometer and reflux condenser. A Schlenk line was connected through the top of the condenser to enable alternation between nitrogen gas, hydrogen gas, and vacuum. The contents of the flask were stirred at 1100 rpm and heated to 308 K. Air from the reactor and the solvent was removed purging the reactor 3 times with nitrogen gas - the pressure was slowly decreased until the solvent started to boil, and the reactor was filled with nitrogen gas quickly. Nitrogen gas was then similarly substituted by hydrogen gas, purging the reactor 3 times. The contents were left stirring under hydrogen atmosphere (ambient pressure) for approximately 30 minutes to ensure the solvent and catalyst were saturated with hydrogen, and that no leak was present in the system (the hydrogen consumption was measured by a 300 mL gas burette). The reaction was started by quickly injecting 1.00 g MBY using a syringe through the septum. Aliquots of approximately 150 µL were taken at regular intervals with the increased sampling rate when the reaction approached 100% conversion (estimated using hydrogen consumption). Analysis of the products was performed using a Varian 430 gas chromatograph equipped with a 30 m Stabilwax® capillary column (Restek). A series of experiments with various stirring rates and catalyst amounts confirmed the absence of external mass transfer limitations, while the calculation of the Weisz-Prater number for the most active catalyst (0.021 and 0.13 for organic and H_2 species, respectively, $\ll 6$) demonstrated that internal mass transfer has a negligible effect on observed kinetics [51].

Conversion of MBY (X_{MBY}) and selectivity to MBE ($S_{MBE,x}$) at different levels of conversion were calculated using the Equations (1-2), where C_{MBY}, C_{MBE}, C_{MBA} and C_x are the concentrations of MBY, MBE, MBA and the concentrations at x% MBY conversion, respectively. These formulae imply that no components other than MBY, MBE and MBA were obtained, which was confirmed by the carbon balance for all reactions of 100 ± 2%.

$$X_{MBY} = \frac{C_{MBE} + C_{MBA}}{C_{MBY} + C_{MBE} + C_{MBA}} \quad (1)$$

$$S_{MBE,x} = \frac{100 \times C^X_{MBE}}{C^X_{MBY} + C^X_{MBE} + C^X_{MBA}} \quad (2)$$

The activity of the catalysts was characterised per mol. of Pd (A) using the average MBY consumption rate in 0-80% MBY conversion interval as in Equation (3), where X^{80}_{MBY} is the MBY conversion close to

80% occurred during the reaction time of t_{MBY}^{80}, C_{MBY}^{80} is the initial MBY concentration, V_{sol} is the solution volume, m_{cat} is the catalyst mass taken with Pd content of ω_{Pd}, and M_{Pd} is the molar mass of Pd.

$$A = \frac{1 - X_{MBY}^{80}}{t_{MBY}^{80}} \frac{C_{MBY}^{0} V_{sol} M_{Pd}}{m_{cat} \omega_{Pd}} \quad (3)$$

Turn-over frequency (TOF) was used to characterise the average activity of the catalyst normalised per active site. The TOF was calculated using Equation (4), where $n_{COuptake}$ is the total molar CO uptake determined by CO chemisorption studies.

$$TOF = \frac{1 - X_{MBY}^{80}}{t_{MBY}^{80}} \frac{C_{MBY}^{0} V_{sol}}{n_{COuptake}} \quad (4)$$

3. Results and Discussion

We adapted the polyol method used by Cable and Shark [49] by performing the reduction of Pd or the co-reduction of Pd and Sn precursors in polyol with the inclusion of TiO_2 or ZnO supports along with the capping agent PVP to control the size distribution of the Pd and Pd_3Sn nanoparticles. The solvent, ethylene glycol, causes the co-reduction of each precursor in the presence of support and the relatively high boiling point (470 K) causes annealing, which induces the formation of the Pd_3Sn alloy phase.

The two supports used, TiO_2 and ZnO were chosen as two common, commercially available materials that are well known for their use as support materials for Pd-based catalysts for hydrogenation reactions [4,52–56]. When supported ZnO, Pd has been shown to offer good catalytic performance in semi-hydrogenation reactions, with selectivities towards MBE reaching around 95% for ZnO supports at 99% MBY conversion [55,56]. Pd nanoparticles supported on TiO_2 were also reported with the selectivity in the range of 60-85 % [3,57,58].

TEM micrographs and particle size distributions of each catalyst are shown in Figure 2. Nanoparticles can be seen on each support material and no nanoparticles greater than 16 nm are observed. The Pd percentages obtained from ICP analysis show close to 2 wt% Pd in each catalyst. Therefore, the vast majority of the Pd used in the synthesis procedure is found in the catalyst with very little Pd lost during or after the synthesis.

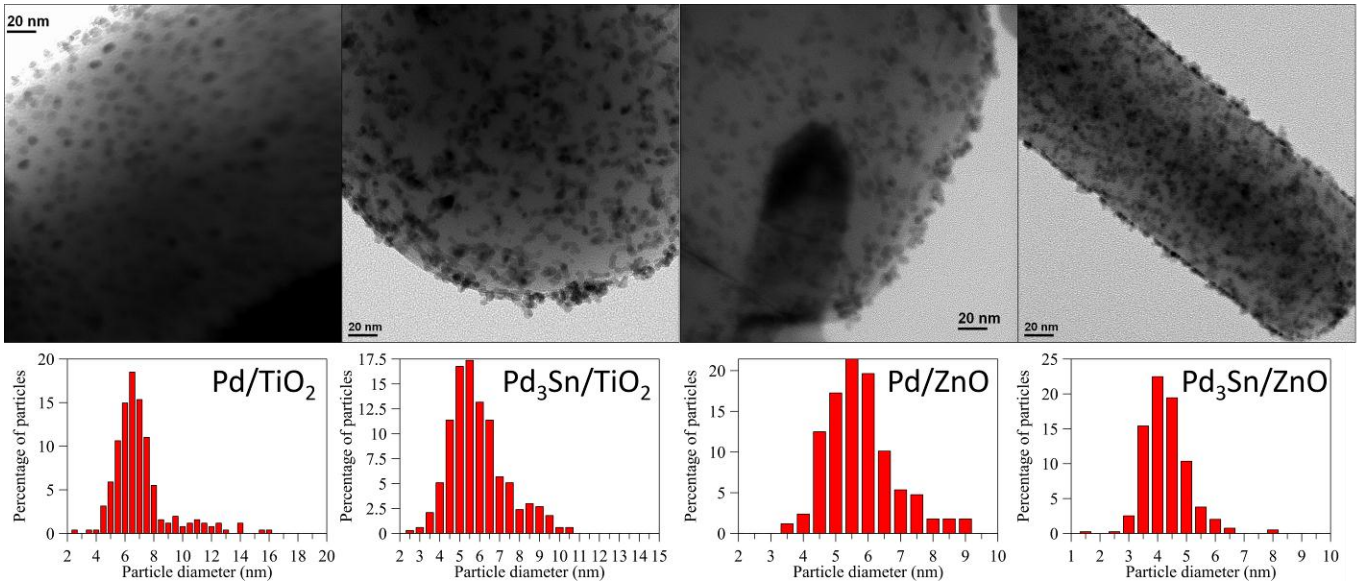

Figure 2. TEM images and particle size distributions of (from left to right) Pd/TiO_2, Pd_3Sn/TiO_2, Pd/ZnO, and Pd_3Sn/ZnO.

Pd_3Sn mean particle size and size distributions (Table 1) are notably lower in Pd_3Sn catalysts than Pd when prepared on the same support in agreement with observations made by Esmaeili *et al.*[44]. Furthermore, the particle size is lower for both Pd and Pd_3Sn catalysts with ZnO support compared to TiO_2 support. The lowest mean particle size (4.1 nm) and size distribution is observed in Pd_3Sn/ZnO. This low particle size may have an effect on the activity of this catalyst compared to the other catalysts, because activity towards semi-hydrogenation has been known to increase sharply above a certain particle size in some cases, due to reaction with the support [59].

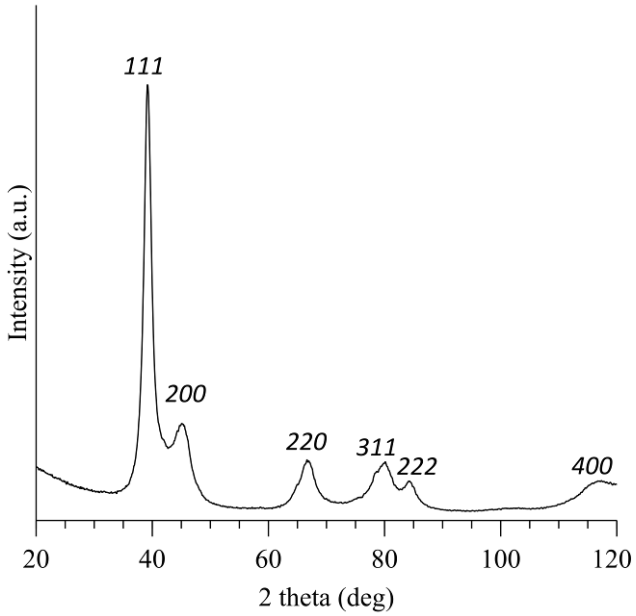

Figure 3. PXRD pattern of unsupported Pd_3Sn.

PXRD and ICP analyses were carried out on Pd_3Sn nanoparticles prepared in the absence of support in order to study the active component of the Pd_3Sn catalysts. The PXRD pattern (Figure 3) was indexed using a face-centred cubic unit cell, in agreement with previous reports on Pd_3Sn [60–65]. Since the PXRD pattern for single-phase Pd is very similar to that of Pd_3Sn, the possibility of overlapping peaks from any pure Pd present in the material cannot be excluded using PXRD alone. However, additional phases, such as SnO_2, Sn metal, or other Pd-Sn compounds that are often found in other works on Pd-Sn materials [37,38,40,44] are not detected. ICP analysis on the same material gave a Pd/Sn ratio of 2.8/1, which is around the lower limit of the Pd_3Sn-phase solid solution reported, the composition of which ranges between $Pd_{2.85}Sn$ and $Pd_{3.26}Sn$, showing a fcc unit cell (space group $Fm\bar{3}m$) throughout [62]. As additional Sn-containing phases are not detected by PXRD, all of the Sn detected by ICP analysis must be incorporated within a Pd_3Sn phase. In this lattice, the Pd and Sn atoms are randomly distributed on the same crystallographic site, hence, the material can be categorised as a random nanoalloy [9]. We have also studied the PXRD patterns for the supported catalysts. However, only diffraction peaks belonging to the support were present and it was impossible to observe any peaks corresponding to Pd or Pd_3Sn due to low particle size (compared to the size of the particles of the support) and low percentage of Pd and Pd_3Sn compared to the support (~ 2 wt%).

The unit cell parameter and the Pd-Pd(Sn) distance were calculated via Rietveld refinement using the GSAS software with the EXPGUI interface [50] and found to be a = 3.949(3) Å, and Pd-Pd(Sn) = 2.7926(13) Å (R_{wp} = 0.098; R_p = 0.074, see Supporting Information) in agreement with the Pd_3Sn model [64].

Recently, Yan et al. [66,67] demonstrated that mechanical strain in catalysts such as Pt/Ni/Cu thin film on a Ti substrate and WC on a polymeric substrate significantly affects the catalytic activity. We considered the possibility of a similar effect in the catalysts studied in this work, however, such an effect is unlikely, as our catalysts are single-phase metal or alloy nanoparticles dispersed on micro sized particles of an oxide support rather than heterogeneous layers.

The CO uptake for each catalyst is shown in Table 1 and tells us how much Pd is available for chemisorption at the catalyst surface. Initially, the CO uptake was measured after performing a pre-reduction treatment in which the catalysts were heated to 573 K in H_2 to remove any residual PVP at the catalyst surface, which is known to be an important factor for CO uptake [68]. However, the CO uptakes were found to be very low compared to those analysed without reduction. This is most apparent when ZnO is used as support, which might be due to a strong metal-support interaction (SMSI) between Pd and

ZnO as a result of the reduction pre-treatment applied before CO uptake measurements were carried out, as observed by Ramos-Fernández *et al.* for the CO uptake of Pt/ZnO [69]. Hence, the calculations for *TOF* (turnover frequency) were done using CO chemisorption data obtained without any pre-reduction treatment being carried out on the catalysts.

Table 1 Comparison of textural properties, elemental analysis and catalyst performance of Pd/TiO_2, Pd_3Sn/TiO_2, Pd/ZnO, and Pd_3Sn/ZnO. $S_{MBE,90}$ and $S_{MBE,100}$ refer to selectivity towards MBE at the onset of conversion of 90 and 100%, respectively. A is the average reaction rate in $mol_{MBY}\ mol_{Pd}^{-1}\ s^{-1}$.

Catalyst	Pd/TiO_2	Pd_3Sn/TiO_2	Pd/ZnO	Pd_3Sn/ZnO
$S_{MBE,90}$ (%)	96.4	97.4	96.2	97.6
$S_{MBE,100}$ (%)	93.7	95.8	93.7	96.1
Mean Pd/Pd_3Sn particle size (nm)	6.8	5.6	5.5	4.1
Particle size standard deviation	2.0	1.4	1.1	0.8
ICP Pd %	1.73	1.97	1.95	1.58
ICP Pd/Sn ratio	n/a	2.9	n/a	2.8
A (s^{-1})	0.42	0.22	0.88	0.06
CO uptake ($\mu mol\ g^{-1}$)[a]	10.8	2.63	0.07	0.29
CO uptake ($\mu mol\ g^{-1}$)[b]	16.1	10.9	3.3	4.9
TOF (s^{-1})	4.3	3.8	49.6	1.9

[a] Catalysts reduced at 573 K in H_2.

[b] Catalysts dried at 373 K in air.

To assess their catalytic performance, the catalysts were tested in batch, liquid phase MBY hydrogenation reactions under identical conditions. The reaction profiles using each catalyst are shown in Figure 4. In all cases, the reaction proceeds by MBY, after which only MBA is produced. This reaction behaviour is expected for Pd-based catalysts as alkynes (MBY) are known to be preferentially adsorbed to the surface of Pd compared to alkene bonds (MBE) [5,6]. The relative formation of MBA compared to MBE is, however, notably lower at all stages of the reaction in the Pd_3Sn catalysts compared to Pd catalysts on the same supports, indicating a lower affinity for alkene adsorption on Pd_3Sn compared to Pd.

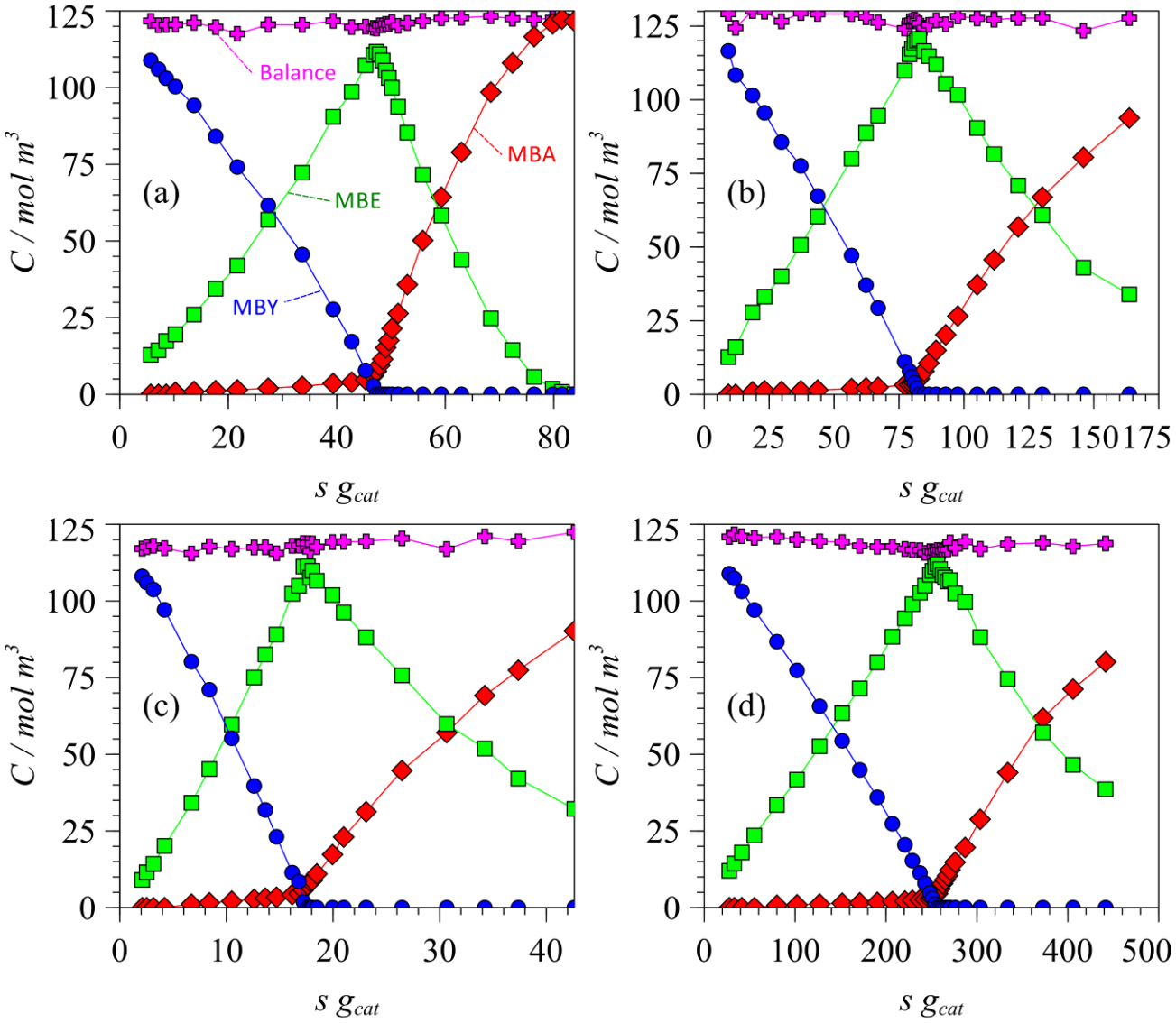

Figure 4. Concentrations of MBY, MBE, and MBA over time (seconds-gram of catalyst) during the semi-hydrogenation reaction at 308 K, 1 atm. H_2 pressure, 0.12 M solution of MBY in hexane. The catalysts are: (a) Pd/TiO_2, (b) Pd_3Sn/TiO_2, (c) Pd/ZnO and (d) Pd_3Sn/ZnO.

The selectivity towards MBE is measured at both 90 and 100% MBY conversion ($S_{MBE,90}$ and $S_{MBE,100}$ in Table 1) but for the purposes of discussion, only $S_{MBE,90}$ is used for a more reliable comparison between catalysts, since the MBA production begins to accelerate slightly before 100% MBY conversion. $S_{MBE,90}$ for each catalyst is shown in Table 1. The catalysts containing Pd_3Sn are $\geq$ 1% more selective at 90% MBY conversion than the corresponding Pd catalyst on the same support. The difference in $S_{MBE,90}$ between Pd/TiO_2 and Pd/ZnO, and between Pd_3Sn/TiO_2 and Pd_3Sn/ZnO is only 0.2%. Therefore in this case, the support cannot be considered the main factor in enhancing the selectivity, which can be attributed to the addition of Sn.

Catalytic activity normalised per mole of Pd (*A*) and per active site (*TOF*) for all catalysts is also listed in Table 1. Activity per mole of Pd in the Pd_3Sn catalysts is lower in all cases compared to the monometallic Pd catalysts, probably due to dilution of Pd with Sn. When measured per active site (*TOF*) the TiO_2-supported catalysts are comparable with a slight decrease in *TOF* from 4.3 s^{-1} (for Pd/TiO_2) to 3.8 s^{-1} (Pd_3Sn/TiO_2). However, *TOF* for Pd/ZnO (49.6 s^{-1}) is an order of magnitude higher than that of any other catalyst, including Pd_3Sn/ZnO (1.9 s^{-1}).

The TOF values for the MBY hydrogenation in the range between 1 and 4 s^{-1} are typical for Pd supported on TiO_2 [28,57], SiO_2 [17] and ZnO [4] nanowire supports. The strong metal-support interactions observed on titania-supported catlaysts, which may increase their activity by a factor of 10, were not observed because we have not performed high-temperature (> 500 ^oC) reduction [53]. Interestingly, the notable increase in TOF for the Pd/ZnO catalysts observed in the current work was also reported previously to be an order of 60 s^{-1}, which is in good agreement with our results [55,70]. However, although selectivity is enhanced, Both *A* and *TOF* are much lower for Pd_3Sn catalysts compared to Pd when ZnO support is used. It is difficult to establish what effect the addition of a second metal has on the interaction between Pd and ZnO support, therefore further work is required to understand the interaction between Pd_3Sn alloy and ZnO support, compared to that between Pd and ZnO.

The mean particle sizes for each catalyst are also listed in Table 1 alongside the values for catalytic activity and selectivity. When the Pd/ZnO and Pd/TiO_2 catalysts are compared, the particle size increases from 5.5 to 6.8 nm. $S_{MBE,90}$ shows little change. However, the activity decreases dramatically. Comparison between Pd_3Sn/ZnO and Pd_3Sn/TiO_2 shows that the mean particle size increases from 4.1 to 5.6 nm and once again $S_{MBE,90}$ exhibits little change, however, in contrast to the Pd based catalysts, the activity dramatically *increases*. Therefore, no obvious correlation can be seen which relates particle size with catalytic performance.

As there is no evidence of Pd/Sn ordering in the FCC lattice of Pd_3Sn, with the distribution of Pd and Sn being random, the enhanced selectivity in Pd_3Sn catalysts may not be entirely attributed to the destruction of Pd ensembles as some literature has suggested for other Pd-Sn catalysts [41,43,44,71]. In fact, there is a 3/1 = Pd/Sn ratio, therefore a large number of Pd ensembles may be intact, hence not achieving a substantial isolation of active sites. Instead, the enhanced selectivity may also be due to a charge transfer from Sn to Pd, suppressing the adsorption of the C=C bond in MBE relative to the C≡C bond in MBY as observed by Hammoudeh and Mahmoud in the selective hydrogenation of cinnamaldehyde [40], leading to very little MBE hydrogenation until almost full conversion of MBY (Figure 4).

4. Conclusions

Pd/TiO_2, Pd/ZnO and the novel catalysts Pd_3Sn/TiO_2 and Pd_3Sn/ZnO were prepared with a one-pot synthesis based on the "polyol method" with the addition of a capping agent (PVP) to control the particle size distribution. All these catalysts showed high activity and selectivity in the semi-hydrogenation of MBY to MBE. However, the new catalysts, in which the catalytically active compound is the Pd_3Sn alloy, are more selective by ≥ 1%, at as low as 90% conversion, compared to the Pd-only based catalysts with the same support. The highest selectivity towards MBE is 97.6% using Pd_3Sn/ZnO. The origin of the enhanced selectivity in Pd_3Sn based catalysts should be further explored, although a plausible explanation based on concomitant factors was offered.

TEM shows nanoparticles on support with Pd_3Sn showing lower mean particle size and less broad size distribution. PXRD analyses of unsupported Pd_3Sn showed that Pd_3Sn is single phase, and is isostructural to Pd metal with Pd and Sn atoms randomly distributed on the same crystallographic position.

Acknowledgement

This work was carried out under an EU funded FP 7 project: Microwave, Acoustic and Plasma Synthesis, Project Number FP70NMP-2012-SMALL-6.

We wish to acknowledge the use of the EPSRC funded National Chemical Database Service hosted by the Royal Society of Chemistry.

We are grateful to Ann Lowry and Bob Knight for TEM and ICP analyses, respectively.

References

[1] W. Bonrath, M. Eggersdorfer, T. Netscher, Catal. Today 121 (2007) 45–57.
[2] W. Bonrath, J. Medlock, J. Schutz, B. Wustenberg, T. Netscher, Hydrogenation in the Vitamins and Fine Chemicals Industry – An Overview, InTech, 2012.
[3] E. V Rebrov, E.A. Klinger, A. Berenguer-Murcia, E.M. Sulman, J.C. Schouten, Org. Process Res. Dev. 13 (2009) 991–998.
[4] L.N. Protasova, E. V. Rebrov, K.L. Choy, S.Y. Pung, V. Engels, M. Cabaj, A.E.H. Wheatley, J.C. Schouten, Catal. Sci. Technol. 1 (2011) 768–77.
[5] G.C. Bond, D.A. Dowden, N. Mackenzie, Trans. Faraday Soc. 54 (1958) 1537.
[6] Á. Molnár, A. Sárkány, M. Varga, J. Mol. Catal. A Chem. 173 (2001) 185–221.
[7] H. Lindlar, Helv. Chim. Acta 35 (1952) 446–450.
[8] J.A. Anderson, J. Mellor, R.K.P.K. Wells, J. Catal. 261 (2009) 208–216.
[9] M. Sankar, N. Dimitratos, P.J. Miedziak, P.P. Wells, C.J. Kiely, G.J. Hutchings, Chem. Soc. Rev. 41 (2012) 8099–8139.
[10] J. Osswald, K. Kovnir, M. Armbrüster, R. Giedigkeit, R.E. Jentoft, U. Wild, Y. Grin, R. Schlögl, J. Catal. 258 (2008) 219–227.
[11] D.C. Huang, K.H. Chang, W.F. Pong, P.K. Tseng, K.J. Hung, W.F. Huang, Catal. Letters 53 (1998) 155–159.
[12] Q. Zhang, J. Li, X. Liu, Q. Zhu, Appl. Catal. A Gen. 197 (2000) 221–228.
[13] A. Hugon, L. Delannoy, C. Louis, Gold Bull. 41 (2008) 127–138.
[14] T. Ward, L. Delannoy, R. Hahn, S. Kendell, C.J. Pursell, C. Louis, B.D. Chandler, ACS Catal. 3 (2013) 2644–2653.
[15] F. Gao, D.W. Goodman, Chem. Soc. Rev. 41 (2012) 8009–8020.
[16] N. Cherkasov, A.O. Ibhadon, E. V. Rebrov, Appl. Catal. A Gen. 515 (2016) 108–115.
[17] N. Cherkasov, A.O. Ibhadon, A. McCue, J.A. Anderson, S.K. Johnston, Appl. Catal. A Gen. 497 (2015) 22–30.
[18] N. Cherkasov, A.O. Ibhadon, E. V. Rebrov, Lab Chip 15 (2015) 1952–1960.
[19] W.G. Menezes, L. Altmann, V. Zielasek, K. Thiel, M. Bäumer, J. Catal. 300 (2013) 125–135.
[20] L. Guczi, Z. Schay, G. Stefler, L.F. Liotta, G. Deganello, A.M. Venezia, J. Catal. 462 (1999) 456–462.
[21] M.B. Boucher, B. Zugic, G. Cladaras, J. Kammert, M.D. Marcinkowski, T.J. Lawton, E.C.H. Sykes, M. Flytzani-Stephanopoulos, Phys. Chem. Chem. Phys. 15 (2013) 12187–96.
[22] J.C.S. Wu, T.-S. Cheng, C.-L. Lai, Appl. Catal. A Gen. 314 (2006) 233–239.
[23] S. Dominguez-Dominguez, A. Berenguer-Murcia, D. Cazorla-Amoros, A. Linares-Solano, J. Catal. 243 (2006) 74–81.
[24] P. Miegge, J.L. Rousset, B. Tardy, J. Massardier, J.C. Bertolini, J. Catal. 149 (1994) 404–413.
[25] J. Serrano-Ruiz, A. Sepulveda-Escribano, F. Rodriguez-Reinoso, J. Catal. 246 (2007) 158–165.
[26] N. Iwasa, M. Takizawa, M. Arai, Appl. Catal. A Gen. 283 (2005) 255–263.
[27] J. Silvestre-Albero, J.C. Serrano-Ruiz, A. Sepúlveda-Escribano, F. Rodríguez-Reinoso, Appl. Catal. A Gen. 292 (2005) 244–251.
[28] E. V Rebrov, E.A. Klinger, A. Berenguer-murcia, E.M. Sulman, J.C. Schouten, Org. Process Res. Dev. (2009) 991–998.
[29] M.W. Tew, H. Emerich, J.A. van Bokhoven, J. Phys. Chem. C 115 (2011) 8457–8465.
[30] M. Varga, Á. Molnár, M. Mohai, I. Bertóti, M. Janik-Czachor, a Szummer, Appl. Catal. A Gen. 234 (2002) 167–178.
[31] B. Coq, F. Figueras, J. Mol. Catal. A Chem. 173 (2001) 117–134.
[32] A. Borodziński, G.C. Bond, Catal. Rev. 50 (2008) 379–469.
[33] Q. He, W. Chen, S. Mukerjee, S. Chen, F. Lufek, J. Power Sources 187 (2009) 298–304.
[34] D. Tu, B. Wu, B. Wang, C. Deng, Y. Gao, Appl. Catal. B Environ. 103 (2011) 163–168.
[35] S.J. Freakley, Q. He, J.H. Harrhy, L. Lu, D.A. Crole, D.J. Morgan, E.N. Ntainjua, J.K. Edwards, A.F. Carley, A.Y. Borisevich, C.J. Kiely, G.J. Hutchings, Science (80-.). 351 (2016) 965–968.
[36] A. Pintar, J. Batista, I. Musevic, Appl. Catal. B Environ. 52 (2004) 49–60.
[37] A. Garron, K. Lazar, F. Epron, Appl. Catal. B Environ. 59 (2005) 57–69.
[38] J. Sa, D. Gasparovicova, K. Hayek, E. Halwax, J.A. Anderson, H. Vinek, Catal. Letters 105 (2005) 209–217.
[39] G. Cárdenas, R. Oliva, P. Reyes, B.L. Rivas, J. Mol. Catal. A Chem. 191 (2003) 75–86.
[40] A. Hammoudeh, S. Mahmoud, J. Mol. Catal. A Chem. 203 (2003) 231–239.
[41] S.H. Choi, J.S. Lee, J. Catal. 193 (2000) 176–185.
[42] C. Breinlich, J. Haubrich, C. Becker, A. Valcarcel, F. Delbecq, K. Wandelt, J. Catal. 251 (2007) 123–130.
[43] E.A. Sales, M. de J. Mendes, F. Bozon-Verduraz, J. Catal. 195 (2000) 96–105.
[44] E. Esmaeili, A.M. Rashidi, A.A. Khodadadi, Y. Mortazavi, M. Rashidzadeh, Fuel Process. Technol. 120 (2014) 113–122.
[45] A.F. Lee, C.J. Baddeley, M.S. Tikhov, R.M. Lambert, Surf. Sci. 373 (1997) 195–209.
[46] K. Kovnir, M. Armbrüster, D. Teschner, T.V. Venkov, L. Szentmiklósi, F.C. Jentoft, a. Knop-Gericke, Y. Grin, R.

Schlögl, Surf. Sci. 603 (2009) 1784–1792.
[47] M. Armbrüster, M. Behrens, F. Cinquini, K. Föttinger, Y. Grin, A. Haghofer, B. Klötzer, A. Knop-Gericke, H. Lorenz, A. Ota, S. Penner, J. Prinz, C. Rameshan, Z. Révay, D. Rosenthal, G. Rupprechter, P. Sautet, R. Schlögl, L. Shao, L. Szentmiklósi, D. Teschner, D. Torres, R. Wagner, R. Widmer, G. Wowsnick, ChemCatChem 4 (2012) 1048–1063.
[48] M. Friedrich, S. Villaseca, L. Szentmiklósi, D. Teschner, M. Armbrüster, Materials (Basel). 6 (2013) 2958–2977.
[49] R.E. Cable, R.E. Schaak, J. Am. Chem. Soc. 128 (2006) 9588–9589.
[50] B.H. Toby, J. Appl. Crystallogr. 34 (2001) 210–213.
[51] M.A. Vannice, Kinetics of Catalytic Reactions, Springer Science+Business Media, New York, 2005.
[52] J.H. Kang, E.W. Shin, W.J. Kim, J.D. Park, S.H. Moon, J. Catal. 208 (2002) 310–320.
[53] P. Weerachawanasak, O. Mekasuwandumrong, M. Arai, S.-I. Fujita, P. Praserthdam, J. Panpranot, J. Catal. 262 (2009) 199–205.
[54] A. Sarkany, Z. Zsoldos, B. Furlong, J.W. Hightower, L. Guczi, J. Catal. 141 (1993) 566–582.
[55] M. Crespo-Quesada, M. Grasemann, N. Semagina, A. Renken, L. Kiwi-Minsker, Catal. Today 147 (2009) 247–254.
[56] N. Semagina, M. Grasemann, N. Xanthopoulos, A. Renken, L. Kiwi-Minsker, J. Catal. 251 (2007) 213–222.
[57] E. V Rebrov, A. Berenguer-Murcia, H.E. Skelton, B.F.G. Johnson, A.E.H. Wheatley, J.C. Schouten, Lab Chip 9 (2009) 503–6.
[58] L.B. Okhlopkova, E. V. Matus, I.P. Prosvirin, M.A. Kerzhentsev, Z.R. Ismagilov, J. Nanoparticle Res. 17 (2015) 1–15.
[59] N. Semagina, A. Renken, L. Kiwi-Minsker, J. Phys. Chem. C 111 (2007) 13933–13937.
[60] H.N. Nowotny, K. Schubert, U. Dettinger, Zeitschrift Fuer Met. 37 (1946) 137–145.
[61] M. Ellner, J. Less Common Met. 78 (1981) P21–P32.
[62] K.L. Shelton, P.A. Merewether, B.J. Skinner, Can. Minerol. 19 (1981) 599–605.
[63] I.R. Harris, M. Cordey-Hayes, J. Less Common Met. 6 (1968) 223–232.
[64] I.R. Harris, G. V Raynor, C.J. Winstanley, J. Less Common Met. 12 (1967) 69–74.
[65] O.T. Woo, J. Rezek, M. Schlesinger, Mater. Sci. Eng. 18 (1975) 163–165.
[66] K. Yan, S.K. Kim, A. Khorshidi, P.R. Guduru, A.A. Peterson, J. Phys. Chem. C 121 (2017) 6177–6183.
[67] K. Yan, T.A. Maark, A. Khorshidi, V.A. Sethuraman, A.A. Peterson, P.R. Guduru, Angew. Chemie 128 (2016) 6283–6289.
[68] I. Simakova, Y. Demidova, J. Glaesel, E. Murzina, T. Schubert, I. Prosvirin, B.J.M. Etzold, D. Murzin, Catal. Sci. Technol. 6 (2016) 8490–8504.
[69] E. V. Ramos-Fernandez, A.F.P. Ferreira, A. Sepulveda-Escribano, F. Kapteijn, F. Rodriguez-Reinoso, J. Catal. 258 (2008) 52–60.
[70] N. Cherkasov, M. Al-rawashdeh, A.O. Ibhadon, E. V Rebrov, Catal. Today 273 (2016) 205–212.
[71] S. Verdier, B. Didillon, S. Morin, D. Uzio, J. Catal. 218 (2003) 288–295.